Characterization of interface debonding in a ceramic–ceramic fibre composite using the indentation method and acoustic emission

D. ROUBY, H. OSMANI
Groupe d'Etudes de Métallurgie Physique et de Physique des Matériaux, U.A. CNRS 341, Insa de Lyon, F69621 Villeurbanne Cédex, France

The indentation method was first used by Marshall [1] to estimate the frictional stress at the fibre–matrix interface in an SiC(Nicalon)/glass–ceramic composite. In the case of frictional sliding at the interface, the effects of the Poisson's ratio of the fibre and of residual thermal stresses were discussed [2, 3] and it was shown that these effects could best be analysed by using an instrumented indentation set-up giving the load–displacement curves by loading and unloading.

An alternate interface behaviour is the perfect bonded case where debonding occurs when critical conditions are fulfilled. In this case, during fibre loading, there is no sliding at the interface and all displacements are fully elastic. For a given critical fibre load, debonding between fibre and matrix occurs, and then frictional sliding can take place.

This type of behaviour under indentation was studied by Mandell *et al.* [4] for glass and graphite fibres in epoxy. The authors concluded that the critical parameter was the interfacial strength (stress condition). Another approach to debonding, based on energy considerations, was previously proposed by Outwater and Murphy [5]; Wells [6] measured the debond stress (critical fibre stress for debonding) in tension of steel wires of varying diameter embedded in epoxy and clearly showed that the debond stress is more accurately predicted by the energy condition.

In this letter we describe debonding experiments by indentation on a ceramic–ceramic composite and compare the observed debond stress with those predicted by the two criteria for debonding (stress condition and energy condition). To do so, the Nicalon fibres are of considerable interest because they exhibit a very large scatter in diameters (say, from 6 to 30 μm) so the effect of fibre radius can be checked for the two conditions.

The indentation apparatus is a standard inverted optical microscope equipped with a microhardness accessory. The displacement of the Vickers indentor is obtained by turning the microscope focus knob. The microhardness accessory permits load measurement optically by observing the displacement of a spider-line in front of a scale in the ocular lens. Acoustic emission (AE) is used to determine the moment of debonding. The AE resonant transducer is fixed on the opposite side of the specimen (Fig. 1); the signal delivered is amplified and processed by a ring-down counter whose value is erased each 0.1 sec. The analogue counting value is converted to frequency and injected, after adequate amplification, into a loud-speaker. Thus an AE event leads to an audible note whose tone is related to the count for this event and then connected to the amplitude of the AE signal.

The material used was an unidirectional SiC(Nicalon)/Mullite composite (fibre volume fraction 0.33) processed by Aérospatiale in France. Special processing conditions gave strong adhesion at the interface between fibre and matrix, so we can study the debonding mechanism. The bars of 5 mm × 8 mm cross-section were cut into pieces of 10 to 12 mm length and clamped between two rods of brass with a square cross-section (Fig. 1). The cross-section perpendicular to fibre direction was polished to a very smooth surface using standard metallographic techniques.

For measuring the debond stress, the following steps are taken.

1. Calibrate the lod by setting dead weights on the indentor.
2. Set the specimen with the AE transducer on the microscope (see Fig. 1).
3. Align the cross-hair of the ocular lens to coincide with the location of the Vickers diamond tip.
4. Choose a given fibre with adequate diameter and surrounding.
5. Measure the fibre diameter ($2r$) the nearest-neighbour fibre distance, with the Vickers apperature (accuracy $\pm 0.5\,\mu$m).
6. Locate the cross-hair at the centre of the fibre.
7. Rotate the Vickers accessory.
8. Slowly turn the focus knob until the diamond tip touches the specimen.
9. Continue to turn the knob to increase the load very slowly and regularly (to be seen in the ocular lens).
10. Stop the loading when an audible signal is heard (in most cases, a small load drop is to be seen at this moment).

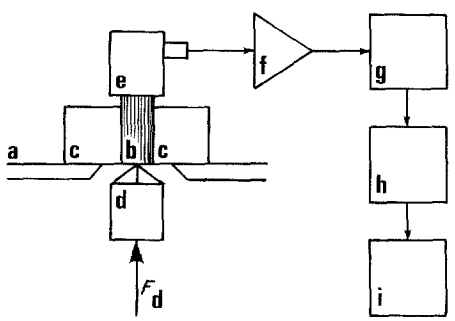

Figure 1 Schematic illustration of the microdebonding apparatus a, Screwplate; b, specimen; c, polishing clamps; d, Vickers indentor; e, acoustic emission transducer; f, main amplifier; g, counter; h, converter; i, loudspeaker.

0261–8028/88 $03.00 + .12

11. Measure the load, F_d, on the scale in the ocular lens (accuracy ± 0.03 N).

12. Rotate the Vickers accessory back and check if there is the correct indent centring and no fibre splitting (splitting occurs for large fibre diameters, more than 20 μm, where the debond load becomes too high).

13. Calculate the debond stress

$$\sigma_d = F_d/\pi r^2 \quad (1)$$

There are two ways of predicting the debond stress. The first is based on the shear-lag analysis [7]. In a model composite consisting of an axial fibre (radius r) surrounded by a cylinder of matrix (radius r'), the shear stress at the interface can be calculated as a function of fibre stress or load. The stress criterion states that debonding occurs when the maximum shear stress at the interface reaches a given critical failure stress, τ_0. For uniform fibre loading a relation between σ_d and interfacial shear strength, τ_0, was found [8]

$$\sigma_d = 2\tau_0(E_f/2G_m)^{1/2}[\ln(r'/r)]^{1/2} \quad (2)$$

where E_f is the Young's modulus of the fibre and G_m the matrix shear modulus. More realistic analysis with finite elements [4] shows that the position of the maximum of shear stress is below the free surface, at a distance depending on the area of fibre which is loaded by indentor contact; the value of maximum shear stress does not depend on this area. It was also shown that the trends between σ_d and τ_0 vary as $(E_f/G_m)^{1/2}$ and that σ_d is experimentally very much less dependent on r'/r (if $r' > 2r$) as predicted by Equation 2. So for our analysis, we assume that σ_d does not depend on r' and r and we have

$$\sigma_d = 2\alpha\tau_0(E_f/2G_m)^{1/2} \quad (3)$$

where α is a factor including the neighbourhood effects of the fibre. We also have

$$F_d = 2\pi\alpha\tau_0 r^2(E_f/2G_m)^{1/2} \quad (4)$$

The second way of predicting σ_d is based on energy balance considerations, as proposed by Outwater and Murphy [5]. The energy criterion states that a debonding crack can propagate along the interface when the energy of the system become lower (work of external forces, elastic energy changes and energy of created surfaces). The resulting expression for debond stress, re-derived by Wells [6] is

$$\sigma_d = (4E_f G_{IIc}/r)^{1/2} \quad (5)$$

or

$$F_d = (4\pi^2 E_f G_{IIc})^{1/2} r^{3/2} \quad (6)$$

where G_{IIc} is the energy needed for mode II crack growth at the interface. It is to be noted that Equations 5 and 6 are obtained by neglecting the elastic energy changes in the matrix.

Figs 2 and 3 show the results obtained for the composite treated respectively at 800 and 1200° C. There is a large scatter arising partly from measuring errors (see the bars on Fig. 1) and also from the material's dispersion, particularly from pre-existing cracks at the interfaces on the polished surface. We

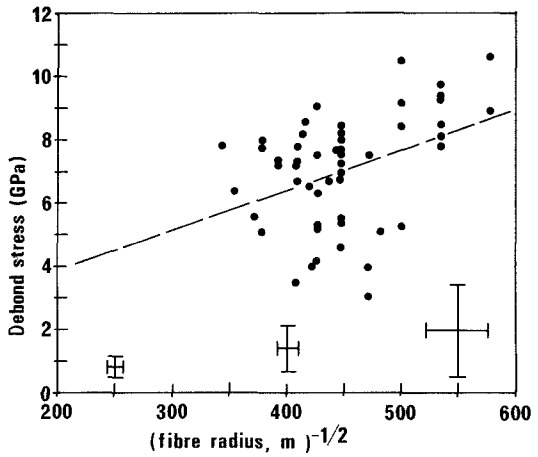

Figure 2 Debond stress σ_d plotted against (fibre radius)$^{-1/2}$ for the specimen treated at 800° C.

have no evidence of a significant effect of the distance between the pushed fibre and the nearest neighbouring one, which can be related to the r'/r ratio. All results given here correspond to a nearest neighbour fibre distance of more than twice the pushed fibre radius.

The results clearly show that σ_d depends on fibre radius. A power law analysis between F_d and r

$$F_d = Ar^n \quad (7)$$

leads to exponent $n = 1.65$ for the 800° C heat treatment and $n = 1.21$ for the 1200° C heat treatment. The exponent is closer to 3/2 (Equation 6) than 2 (Equation 4) and therefore the debonding condition is governed by the energy criterion.

In the σ_d–$r^{-1/2}$ diagrams (shown in Figs 2 and 3), the least-squares fit gives ($\sigma_d > 0$ corresponds to compression)

$$\sigma_d = Br^{-1/2} + \sigma_0 \quad (8)$$

with $B = 0.0127 \times 10^9$ (MKSA), $\sigma_0 = 1.33$ GPa for the 800° C heat treatment and $B = 0.0257 \times 10^9$ (MKSA), $\sigma_0 = -3.82$ GPa for the 1200° C heat treatment. σ_0 can be related to the residual thermal stresses in the fibres. Considering the observed scattering, the values obtained are not very significant. However, we can see that for higher heat treatment temperatures, the fibres are more probably in tension. B corresponds to $(4E_f G_{IIc})^{1/2}$ of Equation 5. Taking $E_f = 200$ GPa we

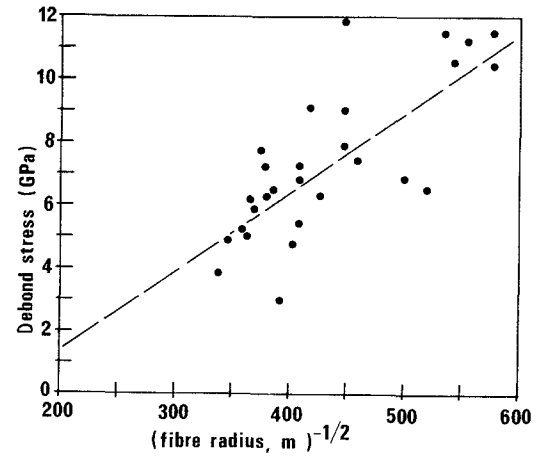

Figure 3 Debond stress σ_d plotted against (fibre radius)$^{-1/2}$ for the specimen treated at 1200° C.

find $G_{IIc} = 202\,J\,m^{-2}$ and $826\,J\,m^{-2}$ for 800 and 1200° C heat treatments, respectively. This difference in G_{IIc} arises from stronger sintering at the interface as the temperature increases. This is also observed on the fractographs where the material treated at higher temperature exhibits less fibre pull-out, due to a stronger interface.

In conclusion, we have shown that AE is a good tool for detecting the debonding event. In spite of the scattering, the results clearly show that in the case of interfacial bonding, the debonding mechanism is governed by the energy release rate and not by a local failure criterion. Finally, this analysis is very easy to perform with an single specimen containing Nicalon fibres, due to the large diameter distribution.

Acknowledgements

We thank Messrs Albughes and Lequertier from Aérospatiale (France) for the materials and for helpful discussions. This paper is based on research sponsored by the CNRS.

References

1. D. B. MARSHALL, *J. Amer. Ceram. Soc.* **67** (1984) C259.
2. K. T. FABER, S. H. ADVANI, J. K. LEE and J.-T. JINN, *ibid.* **69** (1986) C208.
3. D. ROUBY, proceedings of the International Conference "Science of Ceramics 14", Canterbury, UK (1987).
4. J. F. MANDELL, D. H. GRANDE, T. H. TSIANG and F. J. McGARRY in "Composite Materials: Testing and Design (Seventh Conference)", ASTM STP 893, edited by J. M. Whitney (American Society for Testing and Materials, Philadelphia, Pennsylvania, 1986) p. 87.
5. J. D. OUTWATER and L. C. MURPHY, Paper 11C, 24th Annual Technical Conference of Composites (The Society of the Plastics Industry, New York, 1969).
6. J. K. WELLS, PhD thesis, Cambridge University (1982).
7. H. L. COX, *Brit. J. Appl. Phys.* **3** (1952) 72.
8. A. TAKAKU and R. G. C. ARRIDGE, *J. Phys. D Appl. Phys.* **6** (1973) 2038.

Received 7 April
and accepted 28 June 1988